The Astrophysical Journal Letters, 715:L40–L43, 2010 May 20 doi:10.1088/2041-8205/715/1/L40

A MAGNETOHYDRODYNAMIC MODEL FOCUSED ON THE CONFIGURATION OF MAGNETIC FIELD RESPONSIBLE FOR A SOLAR PENUMBRAL MICROJET

T. Magara
Department of Astronomy and Space Science, School of Space Research, Kyung Hee University, 1 Seocheon-dong, Giheung-gu, Yongin, Gyeonggi-do 446-701, Republic of Korea; magara@khu.ac.kr
Received 2010 January 13; accepted 2010 April 19; published 2010 April 30

ABSTRACT

In order to understand the configuration of magnetic field producing a solar penumbral microjet that was recently discovered by *Hinode*, we performed a magnetohydrodynamic simulation reproducing a dynamic process of how that configuration is formed in a modeled solar penumbral region. A horizontal magnetic flux tube representing a penumbral filament is placed in a stratified atmosphere containing the background magnetic field that is directed in a relatively vertical direction. Between the flux tube and the background field there forms the intermediate region in which the magnetic field has a transitional configuration, and the simulation shows that in the intermediate region magnetic reconnection occurs to produce a clear jet-like structure as suggested by observations. The result that a continuous distribution of magnetic field in three-dimensional space gives birth to the intermediate region producing a jet presents a new view about the mechanism of a penumbral microjet, compared to a simplistic view that two field lines, one of which represents a penumbral filament and the other the background field, interact together to produce a jet. We also discuss the role of the intermediate region in protecting the structure of a penumbral filament subject to microjets.

Key words: magnetohydrodynamics (MHD) – methods: numerical – Sun: magnetic topology – sunspots

Online-only material: animation, color figures

1. INTRODUCTION

The solar observing satellite *Hinode* was launched in 2006 September, and since then it has revealed various hidden aspects of solar activity. The sunspot is one of the important targets of observations by *Hinode*, and many new findings on sunspot activity have been reported, such as penumbral structure and dynamics (Bellot Rubio et al. 2007; Jurčák et al. 2007; Katsukawa et al. 2007a; Ichimoto et al. 2007; Borrero & Solanki 2008; Sainz Dalda & Bellot Rubio 2008; Zakharov et al. 2008; Ning et al. 2009; Franz & Schlichenmaier 2009), fine structure of umbrae (Bharti et al. 2007; Kitai et al. 2007; Riethmüller et al. 2008; Watanabe et al. 2009; Sobotka & Jurčák 2009), light bridges (Katsukawa et al. 2007b; Louis et al. 2009; Shimizu et al. 2009), and moving magnetic features (Kubo et al. 2007; Zuccarello et al. 2009; Li et al. 2009).

Among them, a new kind of sunspot activity has been discovered by *Hinode*, named penumbral microjets. This jet-like activity was first reported in Katsukawa et al. (2007a), where the basic properties of penumbral microjets were derived. They are associated with transient brightenings, observed at the boundary of a penumbral filament. Their spatial size is typically 1000–4000 km in length and 400 km in width, while the apparent speed of jet-like motion is about 100 km s^{-1} and the lifetime is about 1 minute. Katsukawa et al. (2007a) found penumbral microjets in the Ca II H line that observes the lower chromosphere with the temperature below 10^4 K. Later, Jurčák & Katsukawa (2008) reported that a penumbral microjet tends to be aligned with the background magnetic field emanating from a sunspot in a relatively vertical direction.

The physical mechanism for producing a penumbral microjet has also been investigated. Some observational works have suggested that a penumbral filament is composed of horizontal magnetic field lines with some twist (Ichimoto et al. 2007) and is surrounded by relatively vertical field lines (Langhans et al. 2005), so the magnetic field is supposed to change direction abruptly near the boundary of a penumbral filament. Magnetic reconnection might occur at that location to produce a jet-like phenomenon (Katsukawa et al. 2007a). Ryutova et al. (2008) present a model where magnetic reconnection and associated shock waves reproduce several observed properties of a penumbral microjet. Sakai & Smith (2008) performed two-fluid simulation in an idealized configuration where vertical and horizontal magnetic flux tubes interact together to produce a jet-like phenomenon. They derived the speed and temperature of a jet.

Following these previous studies, we here investigate a dynamic process of how the configuration of magnetic field responsible for a penumbral microjet is formed in a local penumbral region. We basically follow a model of a penumbra presented by Solanki & Montavon (1993) where a nearly horizontal magnetic flux tube representing a penumbral filament is placed in a stratified atmosphere containing relatively vertical magnetic field (background field). Our result gives a new view that a continuous distribution of magnetic field in three-dimensional space gives birth to the intermediate region where the magnetic field has a transitional configuration between a penumbral flux tube and the background field, and magnetic reconnection occurs in the intermediate region to produce a jet-like structure aligned with the background field, just as the observations indicate. The fact that magnetic reconnection does not involve a penumbral flux tube itself may explain why a penumbral filament can maintain its shape and dynamic state even though a number of microjets occur in the vicinity of that penumbral filament.

2. MODEL DESCRIPTION

We solved a set of magnetohydrodynamic (MHD) equations with uniform gravity in the three-dimensional Cartesian co-

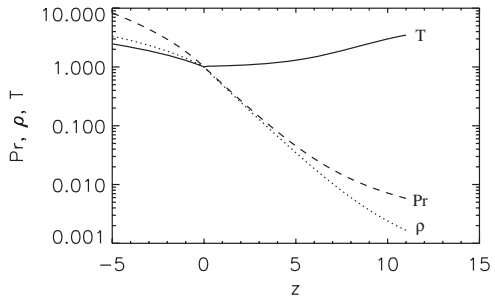

Figure 1. Initial distributions of gas density, pressure, and temperature along the z-axis around the photosphere ($z = 0$), normalized by their photospheric values. The length unit is given by 250 km.

ordinates (x, y, z), where the x- and y-axes form a horizontal plane while the z-axis is directed upward. In the present simulation, these equations have been discretized and integrated with time and space using a modified Lax–Wendroff method (Magara 1998). The whole domain of simulation is $(-16, -16, -6) \leqslant (x, y, z) \leqslant (16, 16, 28)$, and a fine-scale grid $(\Delta x, \Delta y, \Delta z) = (0.1, 0.1, 0.1)$ is applied to an inner domain $(-5, -5, -6) \leqslant (x, y, z) \leqslant (5, 5, 8)$, while the grid size gradually increases outward up to $(\Delta x, \Delta y, \Delta z) = (0.5, 0.5, 0.5)$. The total number of grids is then $N_x \times N_y \times N_z = 181 \times 181 \times 200$.

The plasma is stratified in the z-direction in the same way over the (x, y)-plane under a prescribed temperature profile depending only on z:

$$T(z) = \begin{cases} T_{\rm ph}\left(1 + \frac{z_{\rm ph} - z}{l_{\rm cv}}\right), & \text{for } z < z_{\rm ph} \\ T_{\rm ph} + \frac{(T_{\rm ch} - T_{\rm ph})}{2}\left[\tanh\left(\frac{z - z_{\rm ch}}{l_{\rm ch}}\right) + 1\right], & \text{for } z \geqslant z_{\rm ph}, \end{cases} \quad (1)$$

where $z_{\rm ph} = 0$, $z_{\rm ch} = 10$, $l_{\rm cv} = 3.4$, $l_{\rm ch} = 4$, $T_{\rm ph} = 1$, and $T_{\rm ch} = 5$. Figure 1 shows the initial distributions of the gas pressure, density, and temperature along the z-axis, normalized by their photospheric values. In this simulation, $z_{\rm ph} = 0$ indicates the location of the photosphere, and the units of length, velocity, and time are given by 250 km, 13 km s^{-1}, and 19 s, respectively. The region below the photosphere is weakly unstable for convective motions.

The initial magnetic field is composed of a horizontal flux tube and the background field ($\mathbf{B}^i = \mathbf{B}^f + \mathbf{B}^b$). The background field is given by the potential field that matches the following distribution of vertical magnetic flux at $z = -6$ (bottom boundary)

$$B_z^b(x, y, -6) = B_0 \exp\left(-\left[\frac{(x-6)^2}{40} + \frac{(y+20)^2}{1000}\right]\right), \quad (2)$$

where $B_0 = 9.6$ (the unit of magnetic field is given by 580 G). Since the vertical flux is distributed nonuniformly at the bottom boundary, the background field is somewhat inclined from the vertical direction. On the other hand, the magnetic flux tube is placed horizontally and directed toward the y-direction, expressed by

$$\left(B_x^f, B_y^f, B_z^f\right) = \left(-\frac{\partial \psi}{\partial z}, \alpha\psi, \frac{\partial \psi}{\partial x}\right), \quad (3)$$

and

$$\psi(x, z) = \psi_0 \exp\left(-\left[\frac{(x+4)^2 + (z+1)^2}{5}\right]\right), \quad (4)$$

where $\psi_0 = 36$ and $\alpha = 0.19$. This makes the effective radius of the flux tube about $\sqrt{5} \sim 2.2$, although only the inner part of the flux tube ($r \leqslant 0.7$) has a large axial component, representing a penumbral flux tube.

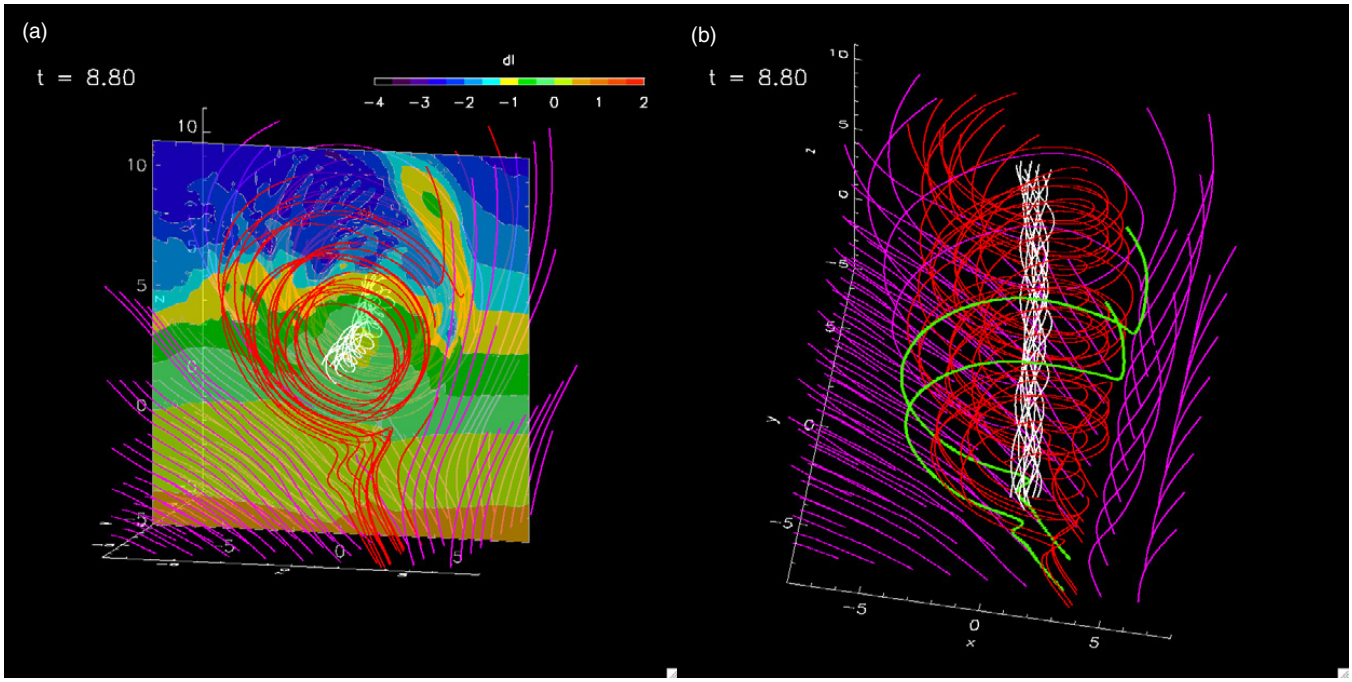

Figure 2. (a) Three-dimensional viewgraph taken at $t = 8.8$, which shows the distributions of magnetic field (colored lines) and gas density (color map at $y = 0$, logarithmic scale) that is normalized by photospheric value. White, red, and purple lines represent a penumbral flux tube, field lines in the intermediate region, and background field, respectively. The length unit is given by 250 km. (b) Similar viewgraph taken at the same time as panel (a) but from a different viewing angle. The green field lines in the intermediate region exert a slingshot effect on plasma.

(A color version and an animation of this figure are available in the online journal.)

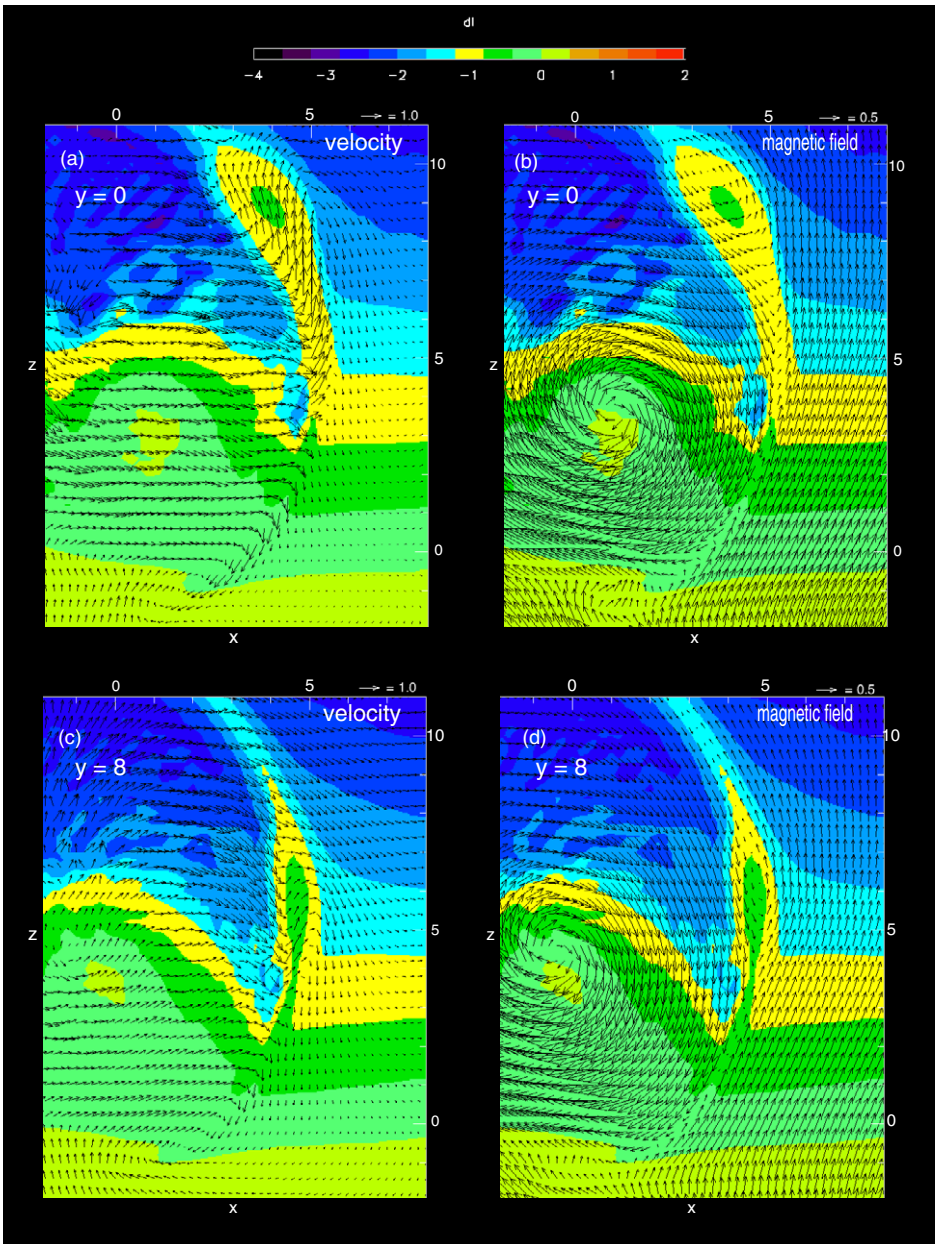

Figure 3. Distributions of velocity field (a, arrows) and magnetic field (b, arrows) at the mid-plane ($y = 0$) where the penumbral flux tube interacts with the background field. Time is $t = 8.8$. The color map shows the distribution of gas density normalized by photospheric value (logarithmic scale). The length unit is given by 250 km. Similar distributions obtained at the same time as in panels (a) and (b) but at a different plane ($y = 8$) are also presented in panels (c) and (d).

(A color version of this figure is available in the online journal.)

In this particular simulation, we assigned a fixed boundary condition at the bottom boundary where all the physical quantities keep initial values, while a free boundary condition is applied to the other boundaries. We put a non-stratified layer near the top and bottom boundaries and also put a wave-damping zone near all the boundaries. The simulation is subject to the so-called numerical resistivity, so pseudo-magnetic reconnection occurs in the region where a discontinuity-like configuration of magnetic field is formed. We therefore lost several important properties of magnetic reconnection such as the Joule heating and reconnection electric field. This issue is discussed in the last section.

3. RESULT

Figure 2(a) shows a snapshot taken at $t = 8.8$ where the distribution of field lines in three-dimensional space and the color map of gas density at a vertical plane ($y = 0$) are presented. Another snapshot obtained at the same time ($t = 8.8$) but from a different viewing angle is also presented in Figure 2(b). The configuration of magnetic field is provided by a weakly twisted flux tube (white lines) representing a penumbral flux tube, the background field (purple lines), and the field lines forming the intermediate region (red lines) where the magnetic field has a transitional configuration between the penumbral flux tube and the background field. Regarding the twist of the penumbral flux tube, it is given by $r/l \sim 0.1$, where $r = 0.7$ is the radius of the penumbral flux tube and $l = 7$ is the axial distance of field lines making one helical turn around the axis of the flux tube. Figure 2(a) clearly shows that a high-density plasma blob is ejected upward in the intermediate region, where the so-called slingshot effect of bending field lines comes into play (see the

green field lines in Figure 2(b) and the attached animation). The length and width of the jet are about 1000 km and 300 km, respectively.

To further investigate the physical process of ejecting a plasma blob, we plotted the velocity field as well as the magnetic field at the two vertical planes, $y = 0$ and $y = 8$. The background field becomes weak toward the positive y-direction, and an interaction between the flux tube and background field starts at smaller y (see Figure 2(b)). In Figures 3(a) and (b), arrows indicate the distributions of velocity field (a) and magnetic field (b) at $y = 0$, while Figures 3(c) and (d) show similar distributions at $y = 8$, all of which are obtained at $t = 8.8$. The color maps in these figures represent the distribution of gas density in logarithmic scale.

Figures 3(a) and (b) show that an interaction between the flux tube and the background field produces a high-speed plasma jet (the speed reaches 20 km s^{-1}) at $y = 0$, while the ejection of a plasma blob has just started at $y = 8$ in Figures 3(c) and (d). In Figure 3(a), the direction of a jet tends to be aligned with the background field (we measured a small velocity component in the y-direction compared to the velocity components v_x and v_z at the jet area). This may be because the field lines involving reconnection nearly lie on the (x, z)-plane. Regarding the configuration of magnetic field, a prominent feature is found: a well-developed jet-like motion is associated with the Petschek-type configuration known in the theory of magnetic reconnection (Petschek 1964) where the acceleration of plasma is mainly driven by the tension force of magnetic field (see Figures 3(a) and (b)). The so-called Sweet–Parker-type configuration of magnetic reconnection (Parker 1957; Sweet 1958) is also found at the early stage of a similar jet-like phenomenon (see Figures 3(c) and (d)). A suggestion from this result is that first the Sweet–Parker-type configuration is formed in the intermediate region, which then evolves toward the Petschek-type configuration to produce a penumbral microjet.

4. DISCUSSION

The present model is focused on the configuration of magnetic field responsible for a penumbral microjet, showing the result that the jet may be produced by magnetic reconnection occurring in the intermediate region formed between a penumbral flux tube and background field. Although it just demonstrates one possible mechanism of a penumbral microjet, not giving a comprehensive explanation for it by using a realistic configuration, the present model gives a new view about the mechanism of a penumbral microjet compared to a simplistic model where two field lines, one of which represents a penumbral flux tube and the other the background field, reconnect to produce a jet. An important result from the present study is that a continuous distribution of magnetic field in three-dimensional space gives birth to the intermediate region between a penumbral flux tube and the background field, and this intermediate region covers, or protects in some sense, a penumbral flux tube. Without this protecting region, a penumbral flux tube might be destroyed via a number of reconnection events, which is well expected in the simplistic model of interacting two field lines mentioned above, although observations show that the structure of a penumbra is quite stable.

On the other hand, we should mention shortcomings of the present model. Since we assume a relatively simple configuration with a single penumbral flux tube floating in the background field which is not entirely realistic, the intermediate region extends widely around the penumbral flux tube (see the red field lines in Figure 2(b)). This, however, cannot be expected in the real circumstance of a penumbral region where a number of penumbral flux tubes coexist densely. In this case, the intermediate region could strongly be compressed and deformed, where the formation of the Sweet–Parker-type configuration leading into the Petschek-type configuration might not be so easy as in the present model. This may explain why we observe penumbral microjets sporadically and intermittently.

We obtained several quantitative properties of a jet-like phenomenon, such that the length and velocity are about 1000 km and 20 km s^{-1}, respectively, the latter of which is almost comparable to the local Alfvén speed. However, those are obtained from an MHD simulation involving pseudo-magnetic reconnection based on numerical resistivity, which ignores key ingredients of the physical process producing a penumbral microjet, such as diffusive effects, partial ionization, and a complicated configuration provided by coexisting penumbral flux tubes. For a better understanding of the physics of penumbral microjets, we certainly need an advanced modeling where at least one of those missing ingredients is included. A complicated configuration containing multiple penumbral flux tubes might be a possible target of our future study.

The author appreciates the referees' useful comments on the Letter. He also wishes to thank the Kyung Hee University for their general assistance. This research was partially supported by the WCU (World Class University) program through the National Research Foundation of Korea funded by the Ministry of Education, Science and Technology (R31-10016). The numerical simulation presented here has been performed using the facilities of the National Institute of Fusion Science in Japan.

REFERENCES

Bellot Rubio, L. R., et al. 2007, ApJ, 668, L91
Bharti, L., Joshi, C., & Jaaffrey, S. N. A. 2007, ApJ, 669, L57
Borrero, J. M., & Solanki, S. K. 2008, ApJ, 687, 668
Franz, M., & Schlichenmaier, R. 2009, A&A, 508, 1453
Ichimoto, K., et al. 2007, Science, 318, 1597
Jurčák, J., & Katsukawa, Y. 2008, A&A, 488, L33
Jurčák, J., et al. 2007, PASJ, 59, 601
Katsukawa, Y., et al. 2007a, Science, 318, 1594
Katsukawa, Y., et al. 2007b, PASJ, 59, 577
Kitai, R., et al. 2007, PASJ, 59, 585
Kubo, M., et al. 2007, PASJ, 59, 607
Langhans, K., Scharmer, G. B., Kiselman, D., Löfdahl, M. G., & Berger, T. E. 2005, A&A, 436, 1087
Li, K. J., Shen, Y. D., Yang, L. H., & Jiang, Y. C. 2009, Acta Astron. Sin., 50, 289
Louis, R. E., Bellot Rubio, L. R., Mathew, S. K., & Venkatakrishnan, P. 2009, ApJ, 704, L29
Magara, T. 1998, PhD thesis, Kyoto Univ.
Ning, Z., Cao, W., & Goode, P. R. 2009, Sol. Phys., 257, 251
Parker, E. N. 1957, J. Geophys. Res., 62, 509
Petschek, H. E. 1964, in The Physics of Solar Flares, ed. W. N. Hess (Washington, DC: NASA), 425
Riethmüller, T. L., Solanki, S. K., & Lagg, A. 2008, ApJ, 678, L157
Ryutova, M., Berger, T., Frank, Z., & Title, A. 2008, ApJ, 686, 1404
Sainz Dalda, A., & Bellot Rubio, L. R. 2008, A&A, 481, L21
Sakai, J. I., & Smith, P. D. 2008, ApJ, 687, L127
Shimizu, T., et al. 2009, ApJ, 696, L66
Sobotka, M., & Jurčák, J. 2009, ApJ, 694, 1080
Solanki, S. K., & Montavon, C. A. P. 1993, A&A, 275, 283
Sweet, P. A. 1958, in IAU Symp. 6, Electromagnetic Phenomena in Cosmical Physics, ed. Bo Lehnert (Cambridge: Cambridge Univ. Press), 123
Watanabe, H., Kitai, R., & Ichimoto, K. 2009, ApJ, 702, 1048
Zakharov, V., Hirzberger, J., Riethmüller, T. L., Solanki, S. K., & Kobel, P. 2008, A&A, 488, L17
Zuccarello, F., Romano, P., Guglielmino, S. L., Centrone, M., Criscuoli, S., Ermolli, I., Berrilli, F., & Del Moro, D. 2009, A&A, 500, L5